Acknowledgment. We wish to thank Mr. L. Levine for assistance in the design of the computer program used in the analysis of the mass spectra.

Supplementary Material Available. Fourteen tables and two figures relating to the mass spectral data and its analysis will appear following these pages in the microfilm edition of this volume of the journal. Photocopies of the supplementary material from this paper only or microfiche (105 × 148 mm, 24× reduction, negatives) containing all of the supplementary material for the papers in this issue may be obtained from the Journals Department, American Chemical Society, 1155 16th Street, N.W., Washington, D.C. 20036. Remit check or money order for \$4.50 for photocopy or \$2.50 for microfiche, referring to code number JACS-75-3942.

References and Notes

(1) Work supported by National Science Foundation (NSF) Grants GP 23267X2 and 38052. Departmental instruments used in this work were supported as follows: NMR spectrometers, Varian A-60 and HA-100D, E. I. duPont de Nemours and Co., Stauffer Chemical Co., Union Carbide Corp., and NSF Grants No. G20207 and GP 8223; Beckman IR-4, E. I. duPont de Nemours and Co.; AEI MS9 mass spectrometer, NSF Grant No. GP 3672.
(2) Preliminary account. H. D. Kaesz, S. A. R. Knox, J. W. Koepke, and R. B. Saillant, *Chem. Commun.*, 477 (1971).
(3) R. Saillant, G. Barcelo, and H. D. Kaesz, *J. Am. Chem. Soc.*, **92**, 5739 (1970).
(4) F. Piacenti, M. Bianchi, P. Frediani, and E. Benedetti, *Inorg. Chem.*, **10**, 2759 (1971).
(5) (a) B. F. G. Johnson, R. D. Johnston, J. Lewis, B. H. Robinson, and G. Wilkinson, *J. Chem. Soc. A*, 2856 (1968); (b) B. F. G. Johnson, J. Lewis, and I. G. Williams, *J. Chem. Soc. A*, 901 (1970).
(6) R. Mason and A. I. M. Rae, *J. Chem. Soc. A*, 778 (1968).
(7) See paragraph at the end of this article regarding supplementary material.
(8) H. D. Kaesz and R. B. Saillant, *Chem. Rev.*, **72**, 231 (1972).
(9) (a) S. W. Kirtley, Dissertation, UCLA, 1972; (b) S. W. Kirtley and H. D. Kaesz, Abstracts, Presented to the 169th National Meeting of the American Chemical Society, Boston, Mass., April 1972, INOR 131; (c) see also discussion of oxygen bridging, R. M. Wing and K. P. Callahan, *Inorg. Chem.*, **8**, 871 (1969).
(10) G. C. Pimentel and A. L. McClellan, "The Hydrogen Bond", W. H. Freeman, San Francisco, Calif., 1960, p 66 ff.
(11) D. B. W. Yawney and F. G. A. Stone, *J. Chem. Soc. A*, 502 (1969).
(12) S. A. R. Knox and F. G. A. Stone, *J. Chem. Soc. A*, 2559 (1969).
(13) (a) B. F. G. Johnson, J. Lewis, and P. Kilty, *J. Chem. Soc. A*, 2859 (1968); (b) C. R. Eady, B. F. G. Johnson, and J. Lewis, *J. Organomet. Chem.*, **57**, C84 (1973).
(14) R. Mason, *Pure Appl. Chem.*, **6**, 31 (1971).
(15) J. R. Moss and W. A. G. Graham, *J. Organomet. Chem.*, **23**, C47 (1970).
(16) J. W. Koepke, J. R. Johnson, S. A. R. Knox, and H. D. Kaesz, see following paper.
(17) S. A. R. Knox and H. D. Kaesz, *J. Am. Chem. Soc.*, **93**, 4594 (1971).
(18) A. J. Canty, A. J. P. Domingos, B. F. G. Johnson, and J. Lewis, *J. Chem. Soc., Dalton Trans.*, 2056 (1974).
(19) (a) Galbraith Laboratories, Knoxville, Tenn.; (b) Heather King, Department of Chemistry, UCLA.
(20) Prepared by mercury lamp irradiation of 10 mmol of $Mo(CO)_6$ in 70 ml of boiling THF until about 80% of the calculated volume of CO is evolved; see similar preparations of $LM(CO)_5$: W. Strohmeier, *Angew. Chem.*, **76**, 873 (1964), and references cited therein such as D. P. Tate, J. M. Augl, and W. R. Knipple, *Inorg. Chem.*, **1**, 434 (1962).
(21) W. Hieber and R. Werner, *Chem. Ber.*, **90**, 286 (1957); see also W. Hieber, W. Beck and G. Braun, *Angew. Chem.*, **72**, 795 (1960).
(22) A. N. Nesmeyanov, K. N. Anisimov, H. Ye. Kolobova, and I. S. Kolomnikov, *Izv. Akad. Nauk SSSR, Otd. Khim. Nauk*, 194 (1963); see also N. Flitcroft, D. K. Huggins, and H. D. Kaesz, *Inorg. Chem.*, **3**, 1123 (1964).

Synthesis and Characterization of Tetraphenylarsonium Tri-μ-hydrido-dodecacarbonyltetraruthenate. Observation of Structural Isomers and Their Rapid Interconversion in a Hydrido–Metal Cluster Anion[1]

J. W. Koepke, J. R. Johnson, S. A. R. Knox, and H. D. Kaesz*

Contribution No. 3289 from the Department of Chemistry, University of California, Los Angeles, California 90024. *Received October 23, 1974*

Abstract: The title compound is synthesized by treatment of $Ru_4H_4(CO)_{12}$ with alcoholic KOH for a short period followed by precipitation with $(C_6H_5)_4AsCl$. Raman spectrum indicates bridging hydrogen through a broad absorption centered at 1442 cm^{-1}, $\Delta\nu_{1/2} \sim 55$ cm^{-1}. Proton magnetic resonance spectra at low temperature reveal the presence in nearly equal concentrations of two isomers one of C_2 or C_{2v} and one of C_{3v} symmetry which are rapidly interconverting. Equilibrium constants and thermodynamic parameters have been obtained in dimethyl ether, tetrahydrofuran, and acetone-d_6 solutions. For the equilibrium: C_2 (or C_{2v}) isomer $\rightleftarrows$ C_{3v} isomer, $K = 1.21$ at $-100°$ in acetone-d_6; $\Delta H = -8.4 \times 10^2$ cal/mol and $\Delta S = -4.5$ cal/(mol deg). Line shape analysis yields activation parameters $\Delta H^{\ddagger} \sim 11$ kcal/mol and $\Delta S^{\ddagger} \sim 0.2$-8 eu for the interchange of hydrogen environments; spin saturation transfer studies indicate this occurs through a combination of intramolecular tautomerism and isomerization pathways.

Whereas substitution of CO predominates in the treatment of hydrido-metal carbonyl cluster complexes with phosphines or phosphites,[2,3] reagents of higher basicity and lower nucleophilicity can lead to deprotonation.[3] In derivatives where the hydrogen atoms are located in positions bridging the metal-metal bonds,[3] they are shielded by the groups bonded to the metals from contact with external reagents. Accordingly, we found the reaction of $Ru_4H_4(CO)_{12}$ with alcoholic KOH to be slow at room temperature. After stirring overnight, however, the hydrido-metal cluster is eventually consumed but only an intractable brown solid showing a broad and featureless absorption in the carbonyl stretching region of the ir is obtained. Further investigations revealed that treatment of the original mixture at 55° for 0.5 hr, followed immediately by the addition of tetraphenylarsonium chloride, gives a red crystalline compound in high yield identified as $[(C_6H_5)_4As][Ru_4H_3(CO)_{12}]$ (**1**).

Infrared spectra for the carbonyl stretching region of **1** in two different solvents and in KBr pellet are given in Table I; the spectrum in acetone solution is shown in Figure 1. These indicate only terminal carbonyl groups, and from the complexity of the pattern one may assume either that a species of low symmetry or that more than one species is present.

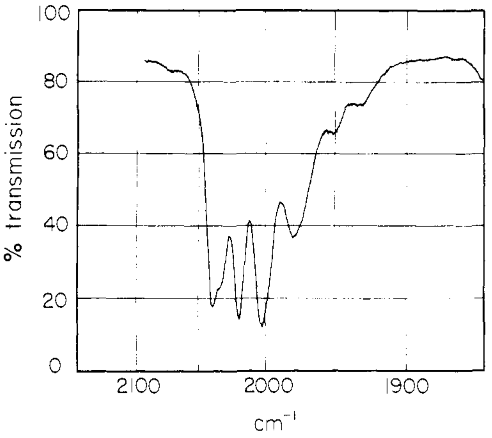

Figure 1. Infrared spectrum of $[AsPh_4][Ru_4H_3(CO)_{12}]$ in the carbonyl region: Beckman IR4, LiF prism; acetone solution.

Raman spectra were attempted; with an exciting line in the red (6328 Å) most samples decomposed. A useful spectrum owing perhaps to fortuitous particle size was obtained on one of the samples and this is shown in Figure 2. The frequencies of the carbonyl bands are listed in Table I while the positions of the other peaks observed are as follows (peaks due to the tetraphenylarsonium ion identified by comparison with the spectrum of $(C_6H_5)_4AsCl$, are marked with an asterisk): 1581 m*, 1442 w ($\Delta\nu_{1/2}$ = 55 cm^{-1}), 1189 w*, 1167 w*, 1088 w*, 1024 m*, 1002 vs*, 672 m*, 617 w*, 484 vs, 429 m cm^{-1}. The broad band at 1442 cm^{-1} is consistent with hydrogen bridging between metals.

Proton NMR spectrum of **1** in acetone-d_6 solution consists at room temperature of two singlets at τ 2.05 and 26.9 whose areas are in the ratio of 20:3. On cooling, the signal at τ 26.9 was observed to change as shown in Figure 3. A limiting spectrum in this region is observed at −95° as shown in the lowest trace in Figure 3 and under optimum resolution at 100 MHz in Figure 4. This consists of three main resonances, a doublet, centered at τ 25.95, a singlet at τ 27.44, and a triplet at τ 29.05 with intensities in the ratio of 2:3.9:1, respectively. The peak at τ 2.05 due to $[(C_6H_5)_4As]^+$ remains unchanged. There is no indication of any other signal from τ 1.70 to 35.0.

The nonintegral relationship of the area under the central peak as compared to the combined areas under the other two peaks suggested to us the presence of two isomeric species one of apparently higher symmetry than the other and possibly differing in polarity. Accordingly, we investigated the limiting spectrum at −100° in solvents of varying dielectric constant. Indeed, the areas under the doublet and the triplet resonances maintained their relative ratio of 2:1 while their total area varied relative to that of the singlet, confirming the presence of two isomers. The one corresponding to the doublet and triplet resonances contains two equivalent hydrogens coupled to a unique hydrogen (J = 2.5 Hz) for which we may deduce structures of C_2 or C_{2v} symmetry, as shown in Figure 5. For the isomer corresponding to the singlet we deduce structures in which all three hydrogen atoms are equivalent such as those shown for C_{3v} symmetry in Figure 5. Alternatively, we might assume this isomer possesses a less symmetric structure but with its hydrogen atoms still undergoing rapid intramolecular exchange at this temperature. Due to limit in solubility in solvents which would permit us to explore this system at lower temperatures, we are able neither to confirm nor to deny this possibility although it seems unlikely to us at present.

Equilibrium constants were calculated from the areas under the peaks in the limiting spectrum and thermodynamic parameters were extracted from the temperature dependence of the equilibrium; the results are presented in Table II and the measurements from which these were derived are given in Tables A, B, and C.[4] The parameters shown in Table II are comparable to those observed for equilibria between rapidly interconverting isomers of different polarity such as rotamers of haloalkanes or cis-trans metal complexes. For example, differences of 888 cal/mol and 1.4 eu were observed for the two rotamers of 2-methylbutane.[5] Enthalpy differences of 0–1900 cal/mol are found in rotamers of haloacetaldehydes[6] and values of 150–720 cal/mol for ΔH and 1.7–5.2 eu for ΔS were found for cis-trans equilibria of dithiocarbamato complexes of iron.[7]

Table I. Ir and Raman Spectra of $[(C_6H_5)_4As][Ru_4H_3(CO)_{12}]$ in Carbonyl Region (cm^{-1})

Infrared			Raman[a]
Acetone solution	THF solution	KBr pellet	Solid
2071 vw	2071 w	2071 vw	2070
2040 s	2037 vs		
2034 s	2032 sh	2033 s (br)	
2019 s	2019 s	2026 vs	
2004 s	2000 s	1990 s	
1978 m		1970 m (br)	1971 vs
		1961 sh	1960 s
		1957 m	
1950 w		1947 m	1947 w
1932 w	1936 w (br)	1939 w	
			1922 vw
		1911 w	1915 w

[a] See Figure 2.

Solvent Effect and Polarity of Isomers. The effect of solvent on the equilibrium data shown in Table II gives us some insight into the structure of the anions. We expect first that ion pairing is going to be negligible due both to the large size of the anion and also the low temperatures at which the equilibria were studied.[8] Evidence regarding this point can be obtained from the infrared spectra. Edgell and Pauuwe[9] have studied the effects of ion pairing on spectra of the salts of $[Cr_2(CO)_{10}]^{2-}$; for the sodium salt in THF solution, the carbonyl absorptions are more complex than expected from symmetry considerations of the isolated anion while the absorptions are observed to simplify in a solvent of higher dielectric constant such as dimethyl sulfoxide. In **1** the infrared spectrum does not change while varying solvent from CH_2Cl_2 to acetone to acetonitrile, covering a range of dielectric constant from 9 to over 30. This indicates that ion pairing is either minimal or, to the extent that it occurs, has little effect on the equilibrium of isomers.

Turning now to the equilibria in Table II, we would expect that the concentration of the more polar isomer is favored as the polarity of the solvent is increased (cf. similar observations for conformer equilibria in substituted 1,3-dioxanes[10] or in equilibria of isomers in hydrido-iron complexes[11]). Through consideration of the need for each metal to achieve a closed valence shell, it is possible to make an assignment for the disposition of negative charge for the possible structures of isomers shown in Figure 5 and thereby to obtain some indication of their relative polarities. For both the C_2 and C_{2v} isomers, the negative charge should be localized on an edge of metals of the tetrahedron, i.e., shared between two metals of the tetrahedron. For C_{3v} isomer A with three hydrogens surrounding one face, the negative charge must be localized on the metal atom opposite that face. For each of the C_{3v} isomers B and C, the charge must be localized on a face, i.e., shared between three metal atoms. Thus a qualitative ordering of polarity from these considerations gives C_{3v} isomer A as the most polar with $C_2 \simeq C_{2v}$ next while C_{3v} isomers B and C would be the least

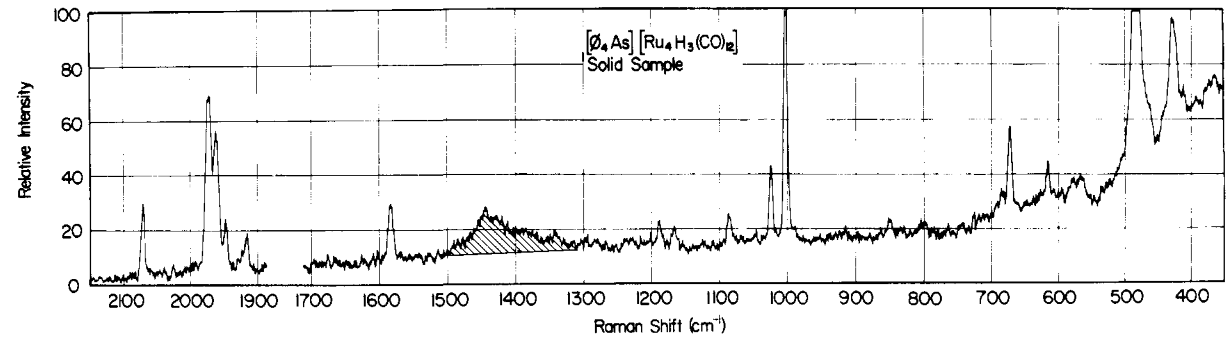

Figure 2. Raman spectrum, Cary 81, 6328 Å exciting line; see Table I for listing of peaks.

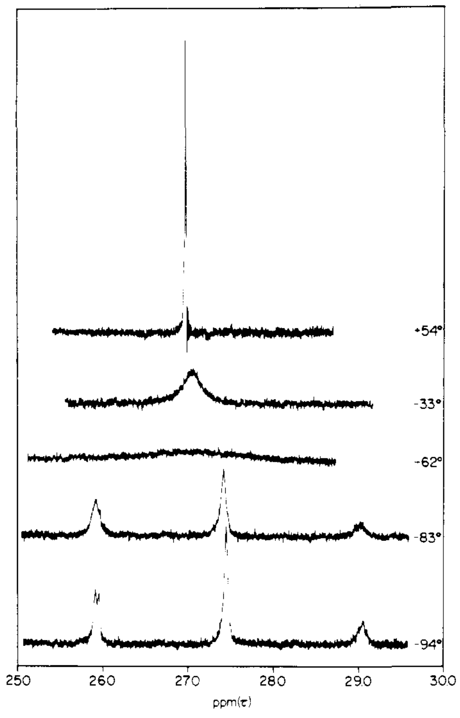

Figure 3. Variable temperature proton NMR spectra of the metal hydride region for $[Ph_4As][Ru_4H_3(CO)_{12}]$: acetone-$d_6$ solution, 60 MHz.

polar. Since the data in Table II indicate that the C_{3v} isomer is favored in solvents of increasing polarity, we conclude that structure A, the most polar, is the prevailing form for that isomer. We have no basis at present on which to select between the C_2 or C_{2v} structures for the other isomer of this anion.

Line Shape Analysis and Pathways of Exchange of Magnetic Environment. There are two elementary processes by which the environment around the hydrogens may become interchanged. The first is intramolecular tautomerism which at present can be distinguished only for the C_2 (or C_{2v}) isomer. Were this process to be occurring alone, as the temperature is raised we would expect to see two signals, the one at τ 27.44 representing the C_{3v} isomer and another at τ 27.0 representing the average of the doublet and triplet in the limiting spectrum. The observed spectra, however, indicate coalescence of all three peaks to one line; this can be produced by rapid exchange between isomers or by a combination of isomer exchange with intramolecular tautomerism. The effects on the line shape in the merging resonances have been calculated for each of these exchange pathways and the results are shown in the two outer series of spectra in Figure 6 together with the corresponding observed spectra at various temperatures displayed in the middle of that figure. If exchange of magnetic environments was occurring solely through exchange between isomers this would require that hydrogen atoms corresponding to the two outer signals in the spectrum could exchange only with those of the central resonance and not with each other; the calculated spectra and rate constants for this process are shown under the heading of "restricted exchange" in Figure 6. Alternatively, if intramolecular tautomerism were occurring together with isomer exchange, this would permit the hydrogen atoms

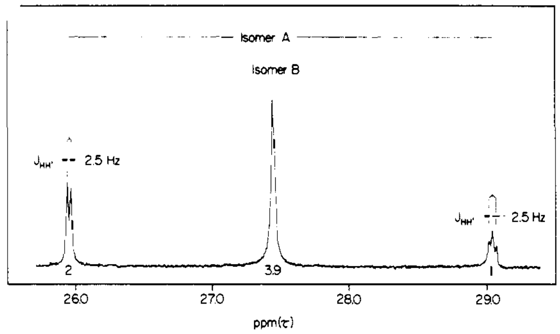

Figure 4. Limiting proton NMR spectrum of the metal hydride region for $[Ph_4As][Ru_4H_3(CO)_{12}]$: acetone-$d_6$ solution, 100 MHz, −95°.

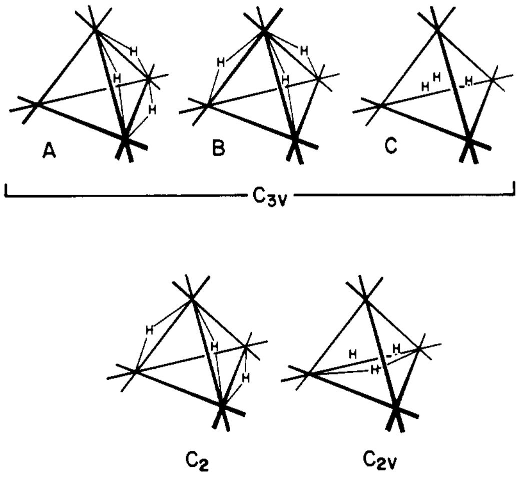

Figure 5. Possible structures of the two isomers of $[AsPh_4][Ru_4H_3(CO)_{12}]$.

Table II. Equilibrium Constants[a] at −100° and Thermodynamic Parameters for Isomers of $[As(C_6H_5)_4][Ru_4H_3(CO)_{12}]$[a] in a Variety of Solvents

Solvent	K_{eq}[a]	ΔH (cal/mol)[a]	ΔS (cal/(mol deg))[a]	Dielectric constant of solvent
CH_3OCH_3	0.995	−826 ± 11	−4.8 ± 0.8	5.02 (25°)
THF	1.06	−772 ± 5	−4.3 ± 0.4	8.20 (20°)
Acetone-d_6	1.21	−842 ± 13	−4.5 ± 1.0	20.7 (25°)

[a] For the equilibrium: C_2 (or C_{2v}) isomer $\rightleftarrows C_{3v}$ isomer.

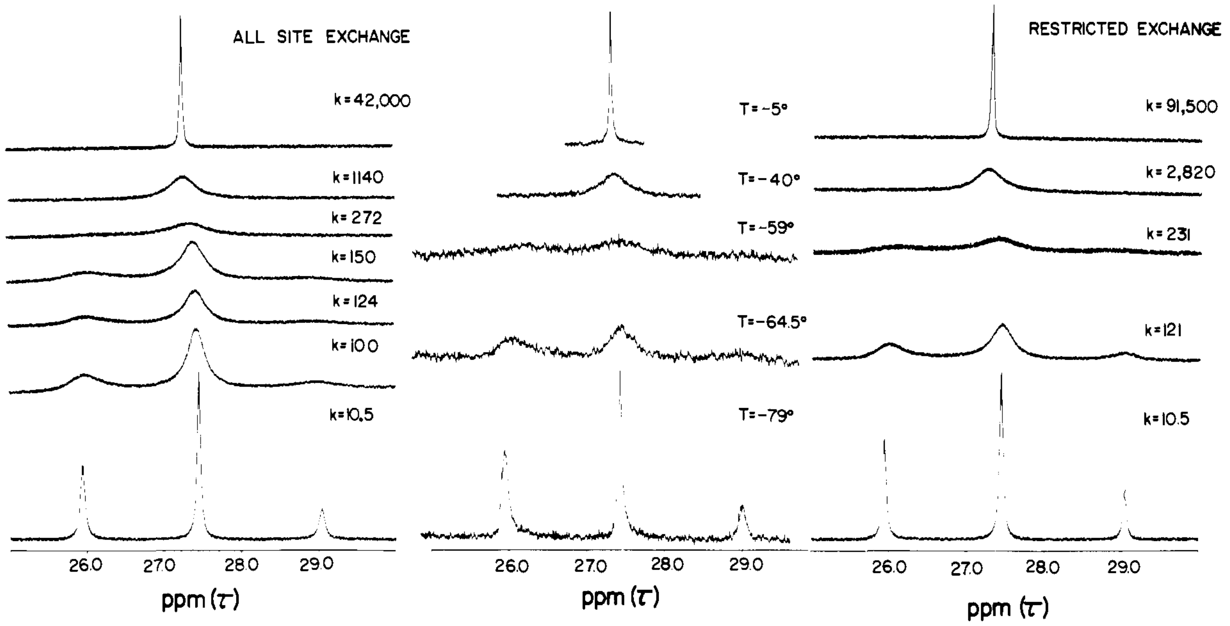

Figure 6. Observed (center) and calculated proton NMR spectra (100 MHz) for the metal hydride region of $[Ph_4As][Ru_4H_3(CO)_{12}]$ at various temperatures. See text for explanation of column headings.

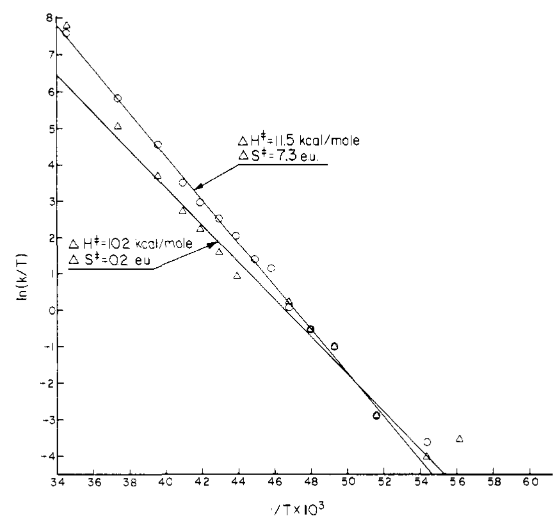

Figure 7. Temperature variation of rate constants calculated for metal hydride resonance spectra under the "all-site" (open triangles) and "restricted" (open circles) exchange pathways. See text for further details.

representing the outer two signals to exchange both with those of the central signal and each other. The calculated spectra and rate constants are displayed under the heading "all-site exchange" in Figure 6. Fuller listings of rate constants pertaining to each of these exchange pathways at various temperatures are given in Table D,[4] and a plot of both sets of data points and least-squares lines derived therefrom are shown in Figure 7. The open circles represent the data for the "restricted" exchange while the open triangles are those for the "all-site" exchange. The points represented by the open circles were used to calculate the steeper of the two least-squares lines while the points represented by open triangles, except for the uppermost on the left, were used to calculate the other straight line.

Little choice can be made from these data between these two exchange processes in the temperature range studied; the evidence indicates that both paths of exchange, i.e., isomerism and intramolecular tautomerism, are competing. While the observed spectrum at −79° is slightly better fit by the spectrum calculated under the "all-site" exchange (see Figure 6) at somewhat higher temperatures, it is difficult to match the observed spectra with this exchange pathway; i.e., when the outer features are matched to the observed spectrum for −64.5° at $k = 100$ or for −59° at $k = 150$, the center feature is not and the reverse of this situation is obtained for the other two calculated spectra, namely, when the central feature is matched to the observed spectrum for −64.5° at $k = 124$ and for −59° at $k = 272$, respectively, the outer features are not. The observed spectra at these two temperatures are better matched by the spectra calculated under the "restricted exchange", $k = 121$ and 131, respectively. Finally, the spectra observed at −40 and −5° can be fit equally well under either mechanism although the data point for the "all-site" exchange pathway at the highest temperature lies far off the least-squares line determined from the other points. The activation parameters for both processes are obviously quite close in this temperature range.

Further evidence for simultaneous traversal over the two exchange pathways is obtained from spin saturation transfer experiments[12] at −80°, see Table III, below. At this temperature, the three resonances of the limiting spectrum are still observed though with some exchange broadening; saturation of the high field resonance brings about a nearly equal reduction in the intensities of the central and the lower field lines, which result would not be obtained if either one or the other of the exchange pathways mentioned above were traversed exclusively. In arriving at this conclusion, of course, we assume that T_1 at the two sites is comparable, which seems quite reasonable in view of the similarity in their chemical environment.

Experimental Section

Materials. The compound $Ru_4H_4(CO)_{12}$ was synthesized as described previously.[13] All other reagents and solvents were those commonly obtained from chemical vendors and were either redistilled from CaH_2 or bubbled with nitrogen for about 5 min to remove dissolved oxygen. Syntheses and initial manipulations were carried out under an inert nitrogen atmosphere using Schlenk glassware. All other manipulations were carried out in air after the product had been found to be air-stable.

Reaction of $Ru_4H_4(CO)_{12}$ with 0.1 *M* KOH in Ethanol. To 400 mg (0.538 mmol) of powdered $Ru_4H_4(CO)_{12}$ was added 7.2 ml of a 0.0837 *M* solution of KOH in absolute ethanol (0.60 mmol of

KOH). Fresh solutions of the ethanolic potassium hydroxide were made up for each new synthesis of the anion to ensure that the concentration of the solution had not changed after the initial weighing of the KOH. The mixture was brought to 55° and over a period of 0.5 hr the solid dissolved to give a deep red solution. To this was added a solution of Ph_4AsCl hydrate (255 mg) in ethanol (approximately 2 ml). On allowing the mixture to cool to room temperature, orange-red crystals formed and were collected. These were washed successively with small portions of ethanol and then hexane. To separate the product from KCl the solids were extracted with dichloromethane, evaporation of which gives 506 mg of $[Ph_4As][Ru_4H_3(CO)_{12}]$ (0.450 mmol), 84% yield based on $Ru_4H_4(CO)_{12}$.

Anal. Calcd for $C_{36}H_{23}AsO_{12}Ru_4$: 38.37; H, 2.09; Found:[14] C, 38.70; H, 2.30.

Measurement of the Isomer Equilibrium in Various Solvents. Three to four spectra were obtained at each temperature and on several different days for each sample to minimize systematic errors in the peak areas. These were integrated by use of a planimeter rather than by electronic means because of the low signal to noise ratio in the spectra. Because of the small area of the triplet peak, the relative population of the isomers was calculated by taking the ratio of the area under the singlet to three-halves of the area under the doublet. The areas on any particular spectrum were found to be reproducible to within about ±4%. Temperature measurements were based on the chemical shift separation of the protons of a methanol sample. For the lower temperatures it was necessary to employ a solution of methanol in Freon, whose frequency separation had been separately calibrated with a thermocouple. The equilibrium constants thus obtained as well as those calculated from a least-squares fit of log K plotted against $1/T$ are presented in Tables A, B, and C.[4] These include the one data point discounted as inconsistent. A total of 14 points between the temperatures of −75 and −108° were used for the calculation in acetone-d_6, 11 points between the temperatures of −86 and −129° in tetrahydrofuran (THF), and 11 points between the temperatures of −88 and −130° for dimethyl ether solutions. The calculated equilibrium constants at −100° and the thermodynamic parameters obtained from the data are shown in Table II. The uncertainties in ΔH and ΔS were calculated statistically from the 95% confidence limit.

Line Shape Analysis. All spectra on which the NMR line shape analysis is based were obtained on a Varian HA-100 instrument equipped with a variable temperature probe. Temperatures were measured with a thermocouple and are considered to be accurate to ±2°. The sample was degassed and sealed under vacuum. The relative population of the two isomers was estimated from the relative areas of the signals below coalescence, extrapolated to higher temperatures.

The proton magnetic resonance spectra employed in this study were obtained in acetone-d_6 to optimize solubility of the title compound at low temperatures. At −95°, the line width of the signals of both Me_4Si and the title compound was broadened to 3.8 Hz because of viscosity. By −85° in this solvent, the line width for Me_4Si had narrowed to 2.0 Hz but observation of the natural line width of the title compound was no longer possible since the features in the limiting spectrum had already begun to broaden due to exchange. In other solvents which do not produce viscosity broadening at −95°, such as CH_3OCH_3, THF, and a 50/50 (volume) mixture of $CFCl_2H\text{-}CH_2{=}CHCl$, the line widths for Me_4Si and for the limiting spectrum of the anion are both 2.0 Hz. It thus seemed appropriate to assign the same natural line width of the title compound in acetone above the temperature of −85° as observed for Me_4Si, namely 2.0 Hz. In any case, the overall spectral features are fairly insensitive to such a small variation in line width. It was also necessary in the calculations to ignore H-H coupling in the C_2 (or C_{2v}) isomer; no provision for such a parameter existed in our program. This omission should, however, also be negligible owing to the small value of the coupling constant (2.5 Hz) compared to the chemical shifts between the coalescing lines (about 300 Hz).

The program used to analyze the spectra was that originally written by Saunders[15a] and made available to us in modified form by Professor F. A. L. Anet.[15b] Values of the rate constant (k) were calculated on an IBM 360-91 computer by an iterative method[15b] based on matching of half-bandwidths by visual comparison as discussed above.

Spin Saturation Transfer. All measurements were made using a Varian HA-100 NMR spectrometer with an external recorder. The HA-100 was also equipped with a variable temperature probe which was accurate to ±2°. Me_4Si was used as an internal reference and also as an internal field/frequency lock; all samples were degassed and sealed under vacuum. Proton magnetic resonance spectra were obtained in acetone-d_6 to maximize solubility of $[Ph_4As][Ru_4H_3(CO)_{12}]$ at low temperatures.

Intensity measurements for these experiments were obtained from peak heights for the resonances under three sets of conditions. First the center of the high field resonance was located at a given temperature. The central or low field resonance was then frequency swept to find the position of maximum absorption. The observation frequency was then locked to the optimum frequency and the external recorder activated to register the height of the peak against time. The peak height was recorded continuously until the signal had stabilized. This intensity is referred to as "normal" peak height. The second set of intensity measurements was made in a similar manner in the spin-decoupling mode of the spectrometer and with the addition of varying amounts of audio power at a position ~200 Hz upfield from the high field resonance. Some decrease in intensity (peak height) is observed as a function of the addition of audio power. Peak heights measured under these conditions are referred to as the "off-resonance" intensities. Finally, peak heights were measured with the same varying amounts of audio power applied at the position of the high field resonance. This measurement yields peak heights "on-resonance", which show the decrease in intensity for these peaks resulting from spin saturation transfer at the various levels of applied audio power. The effects on the lower field and central resonances as varying levels of audio power were applied in irradiating the high field signal of the metal hydride spectrum of $[Ph_4As][Ru_4H_3(CO)_{12}]$ are given in Table III. The values listed are those calculated from the ratio: (peak height "on-resonance" + Δ)/(normal peak height). The correction Δ must be applied to the peak height "on-resonance" to correct for decreases attributable to presence of the audio frequency in the spin-decoupling mode of the spectrometer. In order the check the accuracy of using peak heights instead of areas to measure the intensities of the various resonances, both the central singlet and the low field resonance from isomer A were recorded under the three sets of conditions mentioned above and the areas under the peaks integrated. The same ratios were obtained by this method as shown in Table III.

Due to spin coupling between the low and high field resonances we may expect some signal enhancement of one of these lines from the nuclear Overhauser effect when the other is irradiated. A separate double resonance experiment was carried out at −100° when exchange of protons is essentially quenched; this indicated that signal enhancement in low field line is not greater than 3 or 4% at power levels 25 to 5 dB attenuation and 20 to 25% at 0 dB attenuation, which corrections were applied to the data in calculating the values shown in Table II.

Table III. Heights of the Low Field and Central Peaks upon Irradiation of the High Field Peak for the Metal Hydride Resonances of $[Ph_4As][Ru_4H_3(CO)_{12}]^a$

Attenuation^b (dB)	Peak height of resonances^c	
	Low field	Central
	$T = -80°$	
25	0.98	No effect
20	0.95	0.93
15	0.81	0.90
10	0.66	0.71
5	0.53	0.59
0	0.52	0.57
	$T = -85°$	
15	0.89	. . .
10	0.78	. . .
5	0.81	0.79
0	0.83	0.77

^{a} See spectrum in Figure 6. ^{b} Attenuation of rf power employed for double resonance at high field band. ^{c} Peak height determined as described in the experimental section.

Acknowledgment. Work was supported by National Science Foundation (NSF) Grants GP 23267X2 and 38052. Departmental instruments used in this work were supported as follows: NMR, spectrometers, Varian A-60 and HA-100D, E. I. duPont de Nemours and Co., Stauffer Chemical Co., Union Carbide Corp., NSF Grants No. G20207 and GP 8223; Beckman IR-4, E. I. duPont de Nemours and Co., A.E.I. MS9 mass spectrometer, NSF Grant No. GP 3672; Carey 81 Raman spectrophotometer, NSF Grant No. GP-5240. We would like to thank F. A. L. Anet and J. W. Faller for valuable discussions concerning experimentation and interpretation of spin saturation transfer studies discussed in this work.

Supplementary Material Available. A listing of observed and calculated K_{eq} values for $[Ph_4As][Ru_4H_3(CO)_{12}]$ in acetone-d_6 (Table A), THF (Table B), and CH_3OCH_3 (Table C) and temperature profile of rate constants (Table D) will appear following these pages in the microfilm of this volume of the journal. Photocopies of the supplementary material from this paper only or microfiche (105 × 148 mm, 24 × reduction, negatives) containing all of the supplementary material for the papers in this issue may be obtained from the Journals Department, American Chemical Society, 1155 16th St., N.W., Washington, D.C. 20036. Remit check or money order for $4.00 for photocopy or $2.50 for microfiche, referring to code number JACS 75-3947.

References and Notes

(1) (a) Work presented at the 165th National Meeting of the American Chemical Society, Dallas, Texas, April 8-13, 1973, Abstracts, paper INOR 33; (b) taken in part from the Dissertation of J. W. Koepke, UCLA, Dec 1974.
(2) S. A. R. Knox and H. D. Kaesz, *J. Am. Chem. Soc.*, **93**, 4594 (1971).
(3) H. D. Kaesz, *Chem. Brit.*, **9**, 344 (1973).
(4) See paragraph at the end of this article regarding supplementary material or ref 1b.
(5) R. L. Lipnick and E. W. Garbisch, Jr., *J. Am. Chem. Soc.*, **95**, 6375 (1973).
(6) G. J. Karabatsos, D. J. Fenoglio, and S. S. Lande, *J. Am. Chem. Soc.*, **91**, 3572 (1969).
(7) B. L. Edgar, D. J. Duffy, M. C. Palazzotto, and L. H. Pignolet, *J. Am. Chem. Soc.*, **95**, 1125 (1973).
(8) (a) See discussion in Y. Lim and R. S. Drago, *J. Am. Chem. Soc.*, **94**, 84 (1972), and references cited therein; (b) J. Smid, *Angew Chem., Int. Ed. Engl.*, **11**, 112 (1972).
(9) W. F. Edgell and N. Pauuwe, *Chem. Commun.*, 284 (1969).
(10) E. E. Eliel and O. Hofer, *J. Am. Chem. Soc.*, **95**, 8041 (1973).
(11) P. Meakin, E. L. Muetterties, and J. P. Jesson, *J. Am. Chem. Soc.*, **95**, 75 (1973).
(12) J. W. Faller in "Determination of Organic Structures by Physical Methods", Vol. 5, F. C. Nachod and J. J. Zuckerman, Ed., Academic Press, New York, N.Y., 1973, pp 75-97.
(13) (a) H. D. Kaesz, S. A. R. Knox, J. W. Koepke, and R. B. Saillant, *Chem. Commun.*, 477 (1971); (b) see S. A. R. Knox, J. W. Koepke, M. A. Andrews, and H. D. Kaesz, *J. Am. Chem. Soc.*, preceding paper in this issue.
(14) Heather King, UCLA.
(15) (a) M. Saunders and E. L. Hagen, *J. Am. Chem. Soc.*, **90**, 6881 (1968); (b) adapted for use on IBM 360 machines by P. M. Henrichs, Ph.D. Thesis, U.C.L.A., 1969, with extension to include iterative fitting by William Larson of UCLA Chemistry Department.

Unusual Metalloporphyrin Complexes of Rhenium and Technetium[1]

**M. Tsutsui,*[2a] C. P. Hrung,[2a] D. Ostfeld,[2a] T. S. Srivastava,[2a]
D. L. Cullen,[2b] and E. F. Meyer, Jr.[2b]**

Contribution from the Department of Chemistry, and the Department of Biochemistry and Biophysics, Texas Agricultural Experiment Station, Texas A&M University, College Station, Texas 77843. *Received December 4, 1974*

Abstract: By reaction of dirhenium decacarbonyl, $Re_2(CO)_{10}$, or ditechnetium decacarbonyl, $Tc_2(CO)_{10}$, with mesoporphyrin IX dimethyl ester, H_2MPIXDME, or *meso*-tetraphenylporphine, H_2TPP, monometallic and bimetallic porphyrin complexes of rhenium and technetium were synthesized. Visible spectroscopy indicates that first the monometallic and then the bimetallic porphyrin complex is formed. The monometallic complex of rhenium can further react with either $Re_2(CO)_{10}$ or $Tc_2(CO)_{10}$ to form the homo- and heterodinuclear metalloporphyrin complexes. Structural data for the homodinuclear metalloporphyrin complexes of both rhenium and technetium, $TPP[Re(CO)_3]_2$ and $TPP[Tc(CO)_3]_2$, were obtained by single-crystal X-ray diffraction. Both the rhenium and technetium homodinuclear porphyrins are centrosymmetric complexes having two metals bonded to the porphyrin, one above and one below the plane of the center of the macrocycle while the porphyrin macrocycle is highly distorted. The metal ions are not positioned directly over the center of the macrocycle but are set to one side such that each metal ion is bonded to three nitrogen atoms. There is a small but significant difference in the metal-metal distance, with the Tc-Tc distance being 0.02 Å shorter. The M-M distance (3.101 Å for the Tc complex) though somewhat long for bonding is short enough that some metal-metal interaction may be possible. Due to the observed similarity in both their chemical and physical properties, it was assumed that not only the homo- and heterodinuclear metalloporphyrins but also the monometallic porphyrin complexes of Re and Tc have similar structures. Proton magnetic resonance spectrum of $(H\text{-}TPP)Re(CO)_3$ gave evidence for the proposed structure of the monometallic porphyrin complexes. In the monometallic complexes, the porphyrin acts as a tridentate instead of a tetradentate ligand, while in the bimetallic complexes the porphyrin acts as a hexadentate ligand; both of these are considered nonclassical coordination numbers for the porphyrin ligand. A fluxional character of both Re and Tc monometallic porphyrin complexes was observed by variable-temperature ^1H NMR spectral studies. This fluxional phenomenon is best explained by the intramolecular rearrangement of the metal-carbonyl group among the four ring nitrogen atoms of porphyrin and a concomitant movement of the N-H proton. A novel thermal disproportionation of $(H\text{-}MP)Tc(CO)_3$ to $MP[Tc(CO)_3]_2$ and H_2MPIXDME was also observed. A dissociation and recombination of the metal-carbonyl moieties and the porphyrin ligands between two of the $(H\text{-}MP)Tc(CO)_3$ molecules would seem interpretable for this unusual coordination phenomenon.

There is a growing interest in metalloporphyrins because of the unique nature of the coordination chemistry of these materials[3-8] and also because of their obvious relevance as biological models[9-12] (such as chlorophyll,[13] hemoglobin,[14] cytochrome,[15] and vitamin B_{12}[16,17]). Changes or modification of general porphyrin metabolism are associated with